https://dx.doi.org/10.21577/0103-5053.20200090

J. Braz. Chem. Soc., Vol. 31, No. 11, 2319-2330, 2020
Printed in Brazil - ©2020 Sociedade Brasileira de Química

Article

NO Photorelease from a Ruthenium Complex Assisted by Formation of a Supramolecular Dimer

Douglas B. G. Mateus,[a] Ana Paula L. Batista,[a] Renata L. Rodrigues[b] and Sofia Nikolaou[*,a]*

[a]*Laboratório de Atividade Biológica e Química Supramolecular de Compostos de Coordenação (LABiQSC²), Departamento de Química, Faculdade de Filosofia, Ciências e Letras de Ribeirão Preto, Universidade de São Paulo, Av. Bandeirantes 3900, 14040-901 Ribeirão Preto-SP, Brazil*

[b]*Departamento de Física e Química, Faculdade de Ciências Farmacêuticas de Ribeirão Preto, Universidade de São Paulo, Av. do Café s/n, 14040-903 Ribeirão Preto-SP, Brazil*

This work presents the NO release from compound $[Ru(biq)_2(H_2O)(NO)](PF_6)_3$ (biq = 2,2'-biquinoline) with visible light irradiation (λ_{irrad} = 660 nm), assisted by the low-absorbing photosensitizer $[Ru(biq)_2Cl_2]$. The structure of both compounds were characterized by means of ESI-MS (electrospray ionization mass spectrometry). The NO^+ stretching, ν(NO) = 1995 cm^{-1}, is atypically shifted to higher energy. This observation, along with the $E_{1/2}$ = 0.49 V (*vs*. Ag/AgCl) assigned to the $Ru^{2+/3+}$ redox pair observed for compound $[Ru(biq)_2Cl_2]$ and its photoreactivity in solution suggest that the Ru^{II} ion, when coordinated to two biquinolines, behaves as a hard Pearson acid. Molecular modelling results confirmed the typical geometry distortion of ruthenium-polypyridine complexes bearing sterically hindered ligands. They also suggest the formation of a supramolecular dimer, assembled by weak interaction between biquinoline ligands from each compound, that is claimed to be responsible for the high efficiency of the NO photorelease bimolecular sensitization.

Keywords: NO photorelease, ruthenium biquinoline complexes, bimolecular photosensitization, supramolecular dimer, molecular modelling

Introduction

Ruthenium complexes combined with polypyridines have captured the interest of the scientific community for many years, especially those combined with the 2,2'-bipyridine ligand. A Web of Science survey using the search terms "ruthenium" and "2,2'-bipyridine" yields more than 5650 articles. The $[Ru(bpy)_3]^{2+}$ and $[Ru(bpy)_xL_y]^n$ motifs have been extensively explored over the past 40 years as photo- and/or electroactive units in various forms: as catalysts,[1] electrode modifiers,[2,3] mediators of energy and electron transfer processes,[4,5] in the assembly of supramolecular systems such as dendrimers[6,7] and others,[8] not to mention their biological properties.[9]

Far fewer reports are available on the synthesis and characterization of 2,2'-biquinoline analogs: searching for "ruthenium" and "2,2'-biquinoline" yields modest 74 results. More π-acid ligands than 2,2'-bipyridine are attractive to biological applications, since they lower the energy of the charge transfer states. On the other hand, using bulk ligands such as 2,2'-biquinoline or 2,2'-terpyridine introduces an exacerbated lability of monodentate ancillary ligands. That can make it challenging to handle such complexes in solution but can also be explored to control the delivery of relevant molecules.[10,11]

Given the importance of nitric oxide biological properties,[12] literature reports on numerous organic and inorganic systems capable of releasing NO in a controlled manner. These molecules are called NORMs (NO releasing molecules) or photoNORMs, when NO is released exclusively by light stimulus.[13-15] Specially for coordination complexes, NO photorelease is usually triggered by irradiation with light in the UV region of the electromagnetic spectrum, which has the disadvantage of low skin penetration.[16] Our research group recently discussed[17-19] that, even with an apparent low efficiency

*e-mail: sofia@ffclrp.usp.br
Dedicated to Prof Henrique Eisi Toma on the occasion of his 70th birthday.

of NO photorelease through irradiation with visible light (λ_{irrad} = 660 nm), the low concentrations provided by trinuclear ruthenium nitrosyls of general formula $[Ru_3O(CH_3COO)_6(L)_2NO]PF_6$ (L stands for pyridinic ligands) are able to decrease cellular viability of B16F10 murine melanoma cells and to perform vasorelaxation in pre-contracted rat aorta.

Our group[20,21] also contributed to the strategy of using coordination compounds as photosensitizers to trigger NO release using visible light irradiation, describing the association of mononuclear ruthenium complexes of general formula $[Ru(bpy)_2(aza)L]^n$, where bpy = 2,2'-bipyridine; L = Cl^- or NO^+ and aza = azanaphthalene type ligands. The azanaphthalene type ligands isoquinoline and quinazoline served as anchors for weak interactions in solution in such a way that NO could be delivered with λ_{irrad} > 400 nm from supramolecular dimers. Those previous works demonstrated the viability of using weak interacting units to photorelease nitric oxide efficiently by irradiation in the visible region.

Here we propose to explore again the supramolecular strategy but seeking to use a sensitizer with absorption bands in the therapeutic window. Therefore, this work describes the synthesis, characterization and investigation of solution reactivity of compounds $[Ru(biq)_2Cl_2]$ (**1**) and $[Ru(biq)_2(H_2O)(NO)](PF_6)_3$ (**2**) where biq = 2,2'-biquinoline, Figure 1, as well as the NO photorelease from **2**. As said above, using biquinoline brings the charge transfer band of compound **1** and the solvated species derived from it to lower energies. Besides, biquinoline has planar and hydrophobic portions in its structure, which constitutes potential sites for the arrangement of supramolecular assemblies in solution.

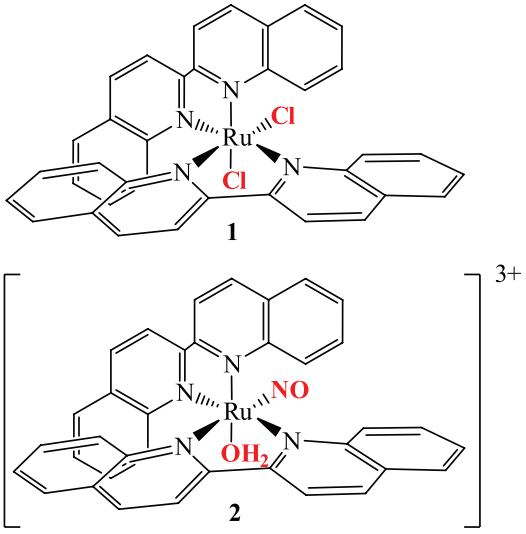

Figure 1. Representation of $[Ru(biq)_2Cl_2]$ (**1**) and $[Ru(biq)_2(H_2O)(NO)](PF_6)_3$ (**2**) structures.

Experimental

General

All reactants and solvents were purchased from Sigma-Aldrich (St. Louis, MO, USA) and were used as received. Elemental analysis was acquired on an Elemental Analyzers CE Instruments model EA 1110. ESI-MS (electrospray ionization mass spectrometry) mass spectra were obtained using an ESI-TOF Mass Spectrometer, ultrOTOFQ model, from methanol solutions acidified with aqueous formic acid (infusion pump 250 μL h^{-1}, positive detection mode). Infrared (IR) spectra was obtained with a Shimadzu Fourier transform infrared (FTIR) spectrophotometer, model Prestige 21, using KBr pellets and 4 cm^{-1} resolution. The electronic spectra were recorded on an HP8453 spectrophotometer, in the region within 200 to 1100 nm, using a 1.00 cm optical path quartz cuvette. The cyclic voltammetry and differential pulse measurements were performed on an AUTOLAB model PGSTAT30 potentiostat/galvanostat system, coupled to a microcomputer. For cyclic voltammetry, acetonitrile (AN) was employed as the solvent, at room temperature and 0.1 mol L^{-1} tetrabutylammonium hexafluorophosphate ($TBAPF_6$) was used as support electrolyte. Differential pulse voltammetry was performed in aqueous solution of 0.1 mol L^{-1} KCl. Both working and auxiliary electrodes were platinum and the reference electrode was Ag/AgCl. Ferrocene was used as an internal standard and the $E_{1/2}$ values were corrected for liquid junction potential.

Continuous light photolysis of the compound $[Ru(biq)_2(NO)(H_2O)](PF_6)_3.H_2O$

A 2.4 × 10^{-5} mol L^{-1} acetonitrile solution of $[Ru(biq)_2(NO)(H_2O)](PF_6)_3.H_2O$ was irradiated with continuous white light (mercury lamp, 250 W) with an optical filter for light under 550 nm. Then, an equimolar acetonitrile solution of the $[Ru(biq)_2(NO)(H_2O)](PF_6)_3.H_2O$ complex and the $[Ru(biq)_2Cl_2]$ sensitizer was irradiated with the same continuous light source, using the 550 nm optical filter. In both cases changes were monitored by electronic spectroscopy.

Laser photolysis of the compound $[Ru(biq)_2(NO)(H_2O)](PF_6)_3.H_2O$

The irradiations were made using a Colibri laser, developed by Quantum Tech. The following laser lines were used: 377 nm (15 mW) and 660 nm (60 mW). Here, the photoinduced gaseous NO release was detected directly

by an ISO-NOP amperometric sensor developed by World Precision Instruments (NOmeter). Since this selective electrode works for aqueous media and the complex is poorly soluble in water, 2.5 mL of a 10^{-4} mol L^{-1} acetonitrile solution of $[Ru(biq)_2(NO)(H_2O)](PF_6)_3.H_2O$ were placed inside a dialysis membrane (Fisherbrand, Cellulose Ester membrane dialysis tubing, 12000-14000 MWCO) sealed with a nylon wire. The dialysis bag was then placed in a beaker containing 17.5 mL of distilled water. The NOmeter electrode is in contact with water (see the Supplementary Information (SI) section, Figure S1, for a scheme of this apparatus). The NO selective electrode has a sensitivity in the range of 1 nM to 20 mM, with relatively short response time, compatible with the proposed pulsed irradiation system. The NOmeter signal was obtained from a Shimadzu CR-7 detection system and transferred to a microcomputer using the DUO.18 v1.1 program.

Synthesis

$[Ru(biq)_2Cl_2]$ (**1**)

The synthesis was performed through an adaptation of the method described in reference.[22] To 5 mL of DMF (*N*,*N*-dimethylformamide), 0.5 g (2 mmol) of biquinoline, 0.26 g (1 mmol) of $RuCl_3.3H_2O$, 0.27 g (0.6 mmol) of LiCl and 0.02 g (0.1 mmol) of ascorbic acid were added. The solution was heated at reflux for 1 h 10 min. After cooling to room temperature, 12 mL of acetone were added to the reaction medium and the mixture was stored in the freezer for one night. The green solid obtained was separated by filtration, washed twice with ice water (2 mL), ethanol (2 mL), and ethyl ether (6 mL). The material was dried in a desiccator containing silica gel. To check for the presence of unreacted biquinoline, few drops of a complex solution were dropped onto an alumina plate and placed under UV light (λ = 365 nm). No luminescense was observed in this way. This procedure afforded 0.3061 g of solid. Reaction yield: 45.0%. Elemental analysis, experimental: C, 63.16%; H, 3.53%; N, 8.17%; $RuC_{36}H_{24}N_4Cl_2$ requires: C, 63.16%; H, 3.53%; N, 8.18%. MS (pESI) *m/z*, calcd. for $RuC_{36}H_{24}N_4$ [**1** – $2Cl^-]^{2+}$ and $RuC_{36}H_{24}N_4Cl$ [**1** – $Cl^-]^+$: 307.0522 and 649.0732, found: 307.0645 and 649.0759, respectively.

$[Ru(biq)_2(H_2O)(NO)](PF_6)_3.H_2O$ (**2**)

The synthesis was based on the method described in reference.[23] To 40 mL of acetonitrile, 48.0 mg (70.2 μmol) of $[Ru(biq)_2Cl_2]$ and 100 mg of the $NOBF_4$ salt (3.4 mmol) were added. Immediately, the solution changed color from green to light orange. The reaction medium was allowed to react under stirring and protected from light for 1 h and then it was evaporated to reduce the amount of solvent to a third. An aqueous saturated NH_4PF_6 solution was added and the mixture was placed in the freezer, yielding a solid precipitated after 25 min. The solid was separated by filtration and it was washed with water and several portions of ethyl ether. The solid was dried under vacuum in a desiccator containing silica gel. This procedure afforded 0.0544 g of solid. Reaction yield: 63.0%. Elemental analysis, experimental: C, 38.67%; H, 2.70%; N, 6.01%; $RuC_{36}H_{28}N_5O_3P_3F_{18}$ requires: C, 38.79%; H, 2.53%; N, 6.28%; IR (KBr) ν / cm^{-1} 3456, 3148, 3091, 3058, 2941, 1995, 1629, 1601, 1538, 1510, 1437, 1389, 1367, 1342, 1312, 1288, 1253, 1216, 1162, 1147, 1108, 967, 922, 878, 841, 791, 780, 751, 558.

Computational methods

The Gaussian 09 program package (revision D.01)[24] was used to obtain the optimized geometry for the bimolecular system in its singlet electronic ground state, at the BP86 D3(BJ)/def2-SVP[25-28] level of theory. This basis set has been used to treat other ruthenium related systems and provided reliable results.[29-32] With the def2-SVP basis set, the 28 inner shell electrons of the ruthenium are modeled by an effective core potential (ECP) (core AOs 1s to 3d), which reduce the basis set size and also account for scalar relativistic effects. This density functional is an affordable and usual approach used to study the structure of related systems.[33,34] Besides, to account for the acetonitrile solvent effect, the continuum solvation model density (SMD) with the integral equation formalism polarizable continuum model (IEF-PCM)[35] was used. The free energy of the complex formation, at 298 K and 1 atm from the above density functional theory (DFT) approach, was obtained using the free energies corrections based on the Grimme[36] rigid-rotor harmonic oscillator model within the GoodVibes[37] program.

To explore the intermolecular interactions on the bimolecular complex optimized geometry, the zeroth-order symmetry-adapted perturbation theory (SAPT0) was applied. The main point of performing this analysis is to get a qualitative understanding of the fundamental physics of nonbonded interactions. Given the molecular size of the bimolecular complex, the wavefunction SAPT0 formalism was chosen because there is a significant computational cost associated with the description of the intramonomer electron correlation in SAPT calculations.[38] In this approach, the intramolecular correlation is ignored, and the intermolecular interactions are described in terms of second-order perturbation theory. This method allows visualizing the interaction energy, in terms of four major components such as electrostatics (E_{Elst}), exchange (E_{Exch}), induction (E_{Ind}), and dispersion (E_{Disp}) terms:[39-41]

$$E_{SAPT0} = E_{Elst} + E_{Exch} + E_{Ind} + E_{Disp} \quad (1)$$

The E_{Elst} term represents the electrostatic interactions between the monomers. The exchange energy may be viewed as a Pauli correction to the electrostatic energy. The induction energy is related to the polarization of one monomer by the other, i.e., how one monomer reacts to the electrostatic field of the other monomer by rearranging its electrons, with an exchange correction to ensure that only Pauli-allowed polarizations occur. Finally, the E_{Disp} term translates the instantaneous charge fluctuations (London dispersion forces) in the system. The current wavefunction SAPT0 method was performed using the Psi4 software[42] along with the def2-SVP basis set and the corresponding auxiliary basis (def2-SVP-JKFIT and def2-SVP-RI)[43,44] to make use of the density-fitting approach. The optimized geometry was visualized using the MacMolPlt[45] software. The SAPT computes the interaction energy directly via a perturbative approach, which provides the interaction energy free from basis set superposition error (BSSE).

Results and Discussion

Structural characterization

Both the sensitizer $[Ru(biq)_2Cl_2]$ (**1**) and the nitrosyl $[Ru(biq)_2(H_2O)(NO)](PF_6)_3.H_2O$ (**2**), as it will be discussed below, presented solution reactivity precluding good NMR (nuclear magnetic resonance) analysis. Therefore, we used ESI-MS mass spectrometry to adress the compounds structure and IR measurements to asses NO coordination (ESI-MS and the IR spectra are available as Figures S2 to S5, SI section).

The ESI-MS mass spectrum was collected from a methanol solution acidified with aqueous formic acid, in order to detect protonated biquinoline in the case of complex fragmentation. In fact, as can be seen in Figure 2, in our experimental conditions the nitrosyl went extensive source-fragmentation, resulting in a spectrum profile dominated by the uncontrolled formation of diverse charged species and precluding the detection of the molecular ion corresponding to the intact complex. However, all of these gas phase ions could be assigned. It was observed three doubly-charged peaks centered at *m/z* 325.1377, 316.0700 and 307.0646, ascribed respectively to the fragment-ions $[Ru(biq)_2(H_2O)_2]^{2+}$ (calculated *m/z* 325.0627), $[Ru(biq)_2H_2O]^{2+}$ (calculated *m/z* 316.0575) and $[Ru(biq)_2]^{2+}$ (calculated *m/z* 307.0522). Peak expansion (Figures S3, SI section) showed a perfect match between the experimental and the theoretical isotopic pattern of mononuclear ruthenium compounds,[46] and $\Delta m/z = 0.5$ corroborates the +2 charge of the gas-phase ions. The distinctive aspect observed here is that, in the gas phase, no fragment containing both biquinoline and NO^+ was observed in the spectrum. This fact suggests that there may be a competition for the electron density of the metal center (Ru^{II} ion) between NO^+ and 2,2'-biquinoline, which is a more acid *N*-heterocyclic ligand than 2,2'-bipyridine, for example.[47] Also, that the Ru-NO^+ bond is weaker than the ones with biquinoline, presumably due to the quelate effect of this last ligand. In solution, the complex is viable because this type of effect can be compensated by the interaction of the complex with solvent molecules, which does not occur in the gas phase. In fact, as will be discussed below, this competition has been observed in other techniques. On the other hand, although the original compound has only one coordinated water molecule, the ESI-MS spectrum displayed an ion (*m/z* 325.1377, Figure 2) with two water molecules in the ruthenium coordination sphere. This observation attests for the high affinity of the $[Ru(biq)_2]$ moiety for water molecules even in gas phase, just as it was observed in solution, which is going to be discussed below.

As expected, a peak corresponding to $[biq-H]^+$ ion (that requires *m/z* 257.1078) is observed. Surprisingly, the species that have dissociated to lose one biquinoline molecule appeared to be associated with one formiate anion, leading to the observation of the singly-charged ions at *m/z* 420.9860 and 438.9998. These gas-phase ions were respectively ascribed to $[Ru(biq)(H_2O)(HCOO)]^+$ (calculated *m/z* 421.0126) and $[Ru(biq)(H_2O)_2(HCOO)]^+$ (calculated *m/z* 439.0231) and the expansion of the corresponding peaks (Figure S4, SI section) shows the match of both theoretical and experimental isotopic distribution for them. The $\Delta m/z = 1$ experimental values show the +1 charge. The mass spectrum is not enough to elucidate whether the formiate anion coordinates or not to the ruthenium ion. Yet, this is likely, since there are vacant positions in its coordination sphere and the solution reactivity of compounds **1** and **2** (see below) revealed that the Ru^{II} ion coordinated to two biquinoline ligands behaves as a Pearson hard acid, having a great affinity for water molecules. This feature is rather consistent with the tendency to react with carboxylic acids.

The infrared spectrum of **2** (Figure S5, SI section) is dominated by the "fingerprint" vibrations of the biquinoline in between 2250 and 400 cm^{-1}, and its strong peak at 841 cm^{-1} is broadened due to superposition with the typical PF_6^- stretching band.[48] Water vibrations are observed as a broad peak centered at 3456 cm^{-1} and, most important, NO stretching band is observed as a symmetrical and very strong peak at 1995 cm^{-1}. In compound **2**, ν(NO) is shifted approximately 50 cm^{-1} to higher energy in relation

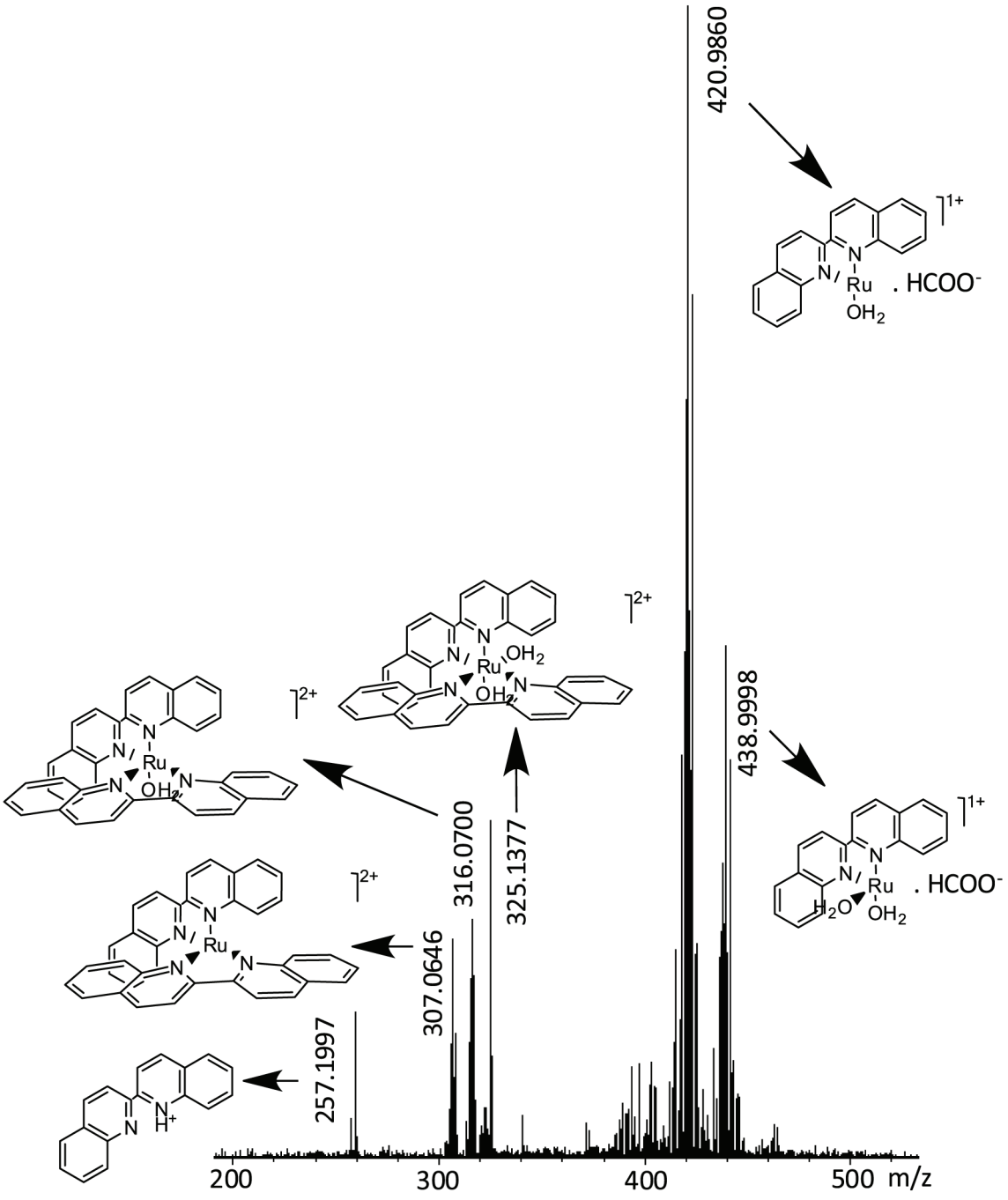

Figure 2. Mass spectrum of compound $[Ru(biq)_2(H_2O)(NO)](PF_6)_3.H_2O$ collected from methanolic solution acidified with aqueous formic acid.

to typical *v*(NO) values observed for the nitrosyl cation coordinated to other ruthenium complexes bearing diimine ligands such as 2,2'-bipyridine.[49] The strengthening of the NO triple bond in **2** is likely due to poorer π-backbonding with the ruthenium central ion. Since 2,2'-biquinoline is more π-acid than 2,2'-bipiridine, for instance,[47] it removes electron density from the metal center, turning it into a site less prone to do strong π-backbonding with other strong π-acceptor ligand such as NO^+. In compound **2**, the biquinoline and the NO^+ ligand are competing for the electron density of the Ru^{II} ion, which ends up behaving like a hard Pearson acid.

An elegant way to address the electronic density of a metal ion is to compare its $E_{1/2}$ values in different coordination complexes. The $E_{1/2}$ values redox process $Ru^{2+/3+}$ observed in the anodic scan of the cyclic voltamamograms of compounds $[Ru(biq)_2Cl_2]$ and $[Ru(biq)_3]^{2+}$ confirm the drastic effect of the biquinoline ligand on the electron density of the metal center. The $[Ru(biq)_3]^{2+}$ moiety displays a redox wave at $E_{1/2}$ = 1.76 V[50] (*vs*. Ag/AgCl),

ascribed to the $Ru^{2+/3+}$ process, showing that it requires a very positive potential to oxidize the Ru^{II} ion. In other words, the π-acceptor biquinoline ligand stabilizes better the lower 2+ oxidation state, making it more difficult to oxidize. Substituting only one biq molecule for two chloro donor ligands in compound **1**, the $E_{1/2}$ value assigned to the $Ru^{2+/3+}$ redox process is more than 1 V negatively shifted to $E_{1/2}$ = 0.49 V (Ag/AgCl, Table 1). This means that, for compound **1**, the central metal ion is much easier to oxidize than it is in the prototype $[Ru(biq)_3]^{2+}$, showing the very strong electronic disturbance promoted by the 2,2'-biquinoline ligands. This observation corroborates the analysis depicted above for the *ν*(NO) shift to higher energy.

Table 1. UV-Vis absorption spectroscopy and cyclic voltammetry data collected for **1** and **2**

	λ_{max} (ε / (L cm^{-1} mol^{-1})) / nm	
	1[a]	**2**[b]
IL[c]		260 (82,595)
IL	350 (43,549)	366 (44,721)
MLCT[d]	732 (6,479)	516 (1,153)
	$E_{1/2}$ / V *vs*. Ag/AgCl[e]	
$Ru^{2+/3+}$	0.49	
$NO^{0/+}$		0.48

[a]Spectrum was collected from a freshly prepared ca. 10^{-5} mol L^{-1} dichloromethane (DCM) solution; [b]spectrum was collected from freshly prepared, ca. 10^{-5} mol L^{-1} acetonitrile solutions; [c]IL: intra-ligand transition; [d]MLCT: metal-to-ligand charge transfer; [e]cyclic voltammograms collected from 0.1 mol L^{-1} $TBAPF_6$ (tetrabutylammonium hexafluorophosphate) freshly prepared ca. 10^{-3} mol L^{-1} acetonitrile solution, at room temperature. Ferrocene was used as internal standard. λ_{max}: maximum absorption wavelength; ε: molar absorptivity coefficient.

Spectroscopic and electrochemical characterization and solution reactivity

Table 1 summarizes the electronic spectroscopy and electrochemical data collected for compounds **1** and **2**.

The electronic spectrum of compound **1** displays the typical metal-to-ligand charge transfer (MLCT) and intra-ligand (IL) transitions at 732 and 350 nm, respectively. This compound presents a distinctive feature that makes it a good candidate for the usage proposed in this study: a large bathochromic shift of the MLCT band. Typically, mononuclear ruthenium polypyridine complexes display their MLCT band in the visible region, up to 600 nm.[50-52] Being 2,2'-biquinoline a π-acid ligand, its π* levels are lower in energy compared to 2,2'-bipyridine. Also, in compound **1**, electronic density donation from the chloro ligands should raise the energy of the dπ levels of the metal center. Both electronic effects contribute to the bathochromic shift observed on the MLCT band.

Due to different skin penetration capacity of light for each wavelength, photosensitizers with lower energy absorptions are more effective to be employed for therapeutic purposes. This property allows the planning of using a compound such as **1** as photosensitizer, in such a way that irradiation with low energy light might trigger NO photorelease. In fact, this would not be possible by direct irradiation of compound **2**. As shown in Table 1, coordination of NO^+ to the metallic center shifts absorption bands to blue and complex **2** shows only a residual absorption in the visible region at 516 nm.

The ability of NO^+ to stabilize the Ru^{II} ion is typical in nitrosyl complexes, in such a way that the $E_{1/2}$ value of the $Ru^{2+/3+}$ redox pair, especially for complexes coordinated to *N*-heterocyclic ligands, occurs beyond the working window of ordinary solvents such as dry acetonitrile. In these cases, only the monoelectronic reduction process of NO^+ is observed.[53] For compound **2**, this occurs as a reversible wave at $E_{1/2}$ = 0.48 V *vs*. Ag/AgCl. To confirm this assignment, we performed a differential pulse voltammetry of **2** in aqueous media in the presence and in the absence of ascorbic acid. The redox wave centered at 0.48 V vanishes upon the addition of the reducing agent, consistently with the chemical reduction of the coordinated NO^+ to NO^0 (both voltammograms are available as Figure S6, SI section).

While the use of biquinoline complexes with low energy absorption bands as photosensitizers for photodynamic therapy is advantageous, the coordination of such chelate introduces a great lability to the monodentate ancillary ligands. Bulky ligands such as biquinoline originate significant geometry distortions from the ideal octahedral geometry of the metal center, leading to poorer overlap with the d orbitals. The main consequence of this is that such ligands exert smaller crystal field splitting. With a smaller split, the ^{3}LF levels have their energy decreased, then they can be thermally populated from the photochemically generated ^{3}MLCT levels. Once populated, their electron density is increased, weakening the sigma bonds with the ligands coordinated to the metallic center. Thus, these low lying ^{3}LF levels are responsible for the exacerbated lability of the monodentate ancillary ligands in sterically hindered ruthenium-polypyridine compounds.[54-60]

For this reason, we investigated the solution reactivity of compounds **1** and **2** under different luminosity conditions and different solvents. As can be seen in Figure 3a, even when we recorded the cyclic voltammograms of **1** with a freshly prepared solution, it was observed two redox processes in the anodic scan, centered at $E_{1/2}$ = 0.49 and 1.04 V (*vs*. Ag/AgCl) of roughly the same intensity. We assigned these waves to the oxidation of the ruthenium ion

in compound **1** and in the solvated species, respectively. Consistently, the chloro ligand should stabilize better the Ru^{III} ion in comparison with acetonitrile, requiring less energy to oxidize it and hence, lowering the $E_{1/2}$ value of the $Ru^{2+/3+}$ process to 0.49 V in comparison to the value of 1.04 V observed for the same redox process in the solvated species. To confirm this assignment, a cyclic voltammogram was collected for a solution of **1** allowed to stand under ambient light for 6 h. After this time interval, it is possible to verify the significant increase in intensity for the wave at 1.04 V in comparison to the one at 0.49 V, confirming the substitution of the chloro ligands for the acetonitrile coordinating solvent (Figure 3b).

Figure 4a presents the electronic spectra of **1** in dry dichloromethane (DCM), dry acetonitrile (AN) and acetonitrile following the addition of water excess. Under ambient luminosity, we observed that dissolving compound **1** in a non-coordinating solvent such as DCM provides a green solution (λ_{max} = 732 nm) which remains unchanged after long periods. Dissolution in AN lead to color changes that are completed after 6 h, affording a blue solution (λ_{max} = 604 nm). Compound **1** is very little soluble in water. Then, we have prepared another solution in acetonitrile and to that we have added an excess of water. The H_2O addition promotes immediate solution color change to pink (λ_{max} = 534 nm). These changes are consistent with the exchange of the chloro ligands for solvent molecules, to afford the species $[Ru(biq)(AN)_2]^{2+}$ (blue) and $[Ru(biq)(H_2O)_2]^{2+}$ (pink) from the original green $[Ru(biq)_2Cl_2]$ compound. Further, the addition of a saturated aqueous solution of LiCl to an acetonitrile solution of **1** does not lead to color changes. Instead, we

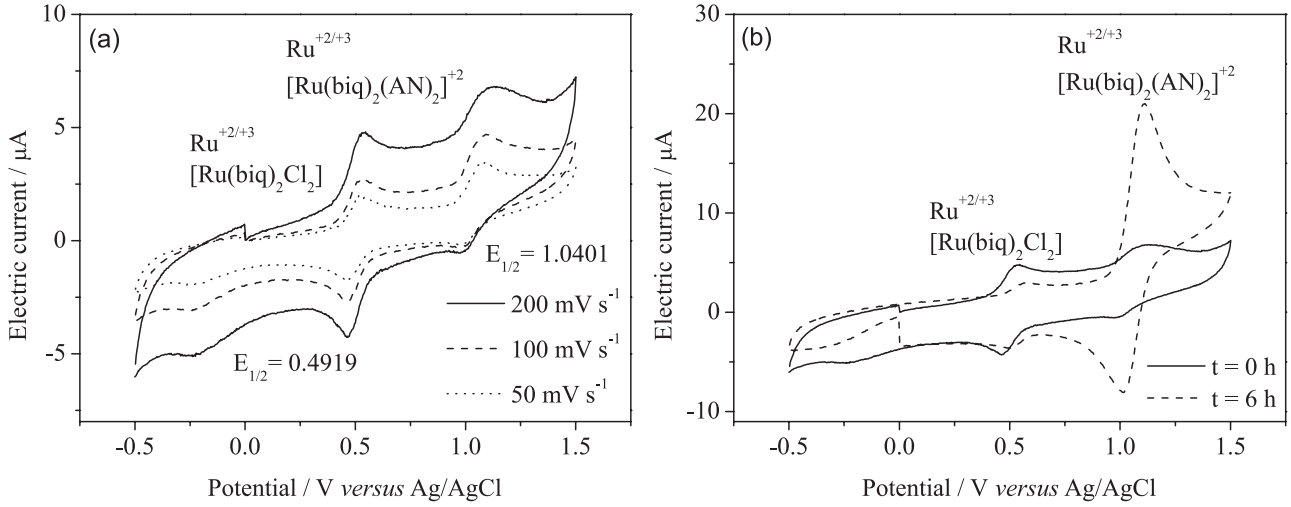

Figure 3. (a) Cyclic voltammetry of the compound **1** recorded from a freshly prepared solution; (b) comparison of the 200 mV s^{-1} scan of the freshly prepared solution with the cyclic voltammogram of a solution left to stand under ambient light for 6 h (0.1 $TBAPF_6$ acetonitrile solutions, anodic scan).

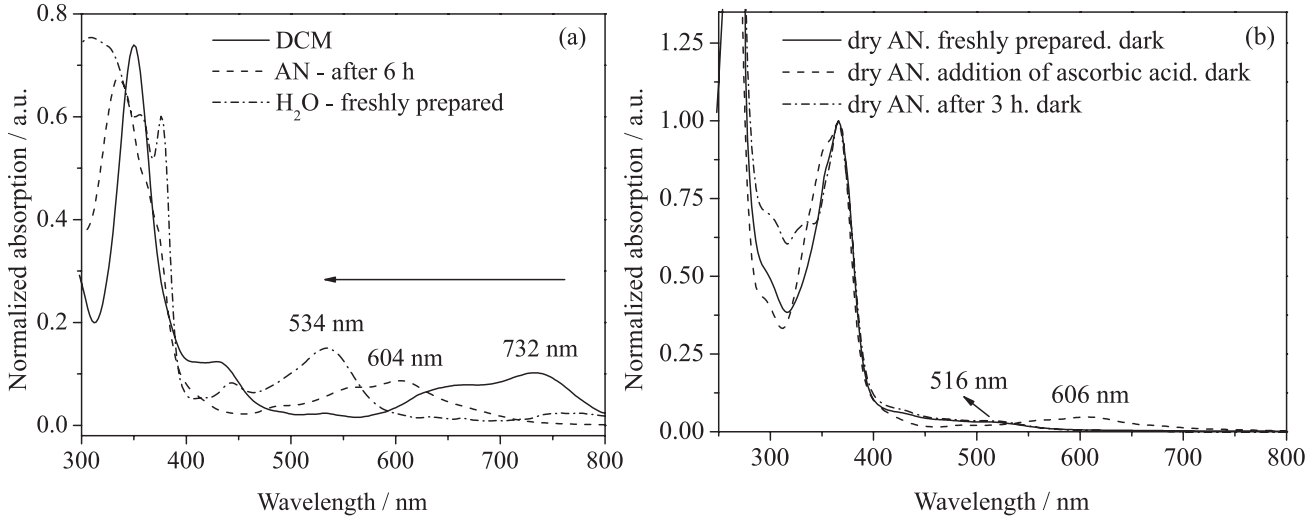

Figure 4. (a) Electronic spectrum of **1** in dichloromethane (DCM), in acetonitrile (AN) after 6 h under ambient light, in acetonitrile with addition of water; (b) dark reactivity of the nitrosyl **2**, in dry AN solution.

observed the formation of a green solid, ascribed to the precipitation of **1**, whose solubility is probably decreased by the presence of the electrolyte in solution. Dilution of the pink mixture AN:H_2O with more acetonitrile does not restore the green color, showing that in the presence of water, even with an excess of AN, compound **1** has more affinity for water molecules.

The reactivity depicted above and summarized in Scheme 1, demonstrated the high affinity for water of the Ru^{II} ion in compound **1**. Being water a harder Pearson base compared to acetonitrile, this affinity reveals a more acidic character of this Ru^{II} ion, probably due to coordination of the very strong π-accepting biquinoline ligand.

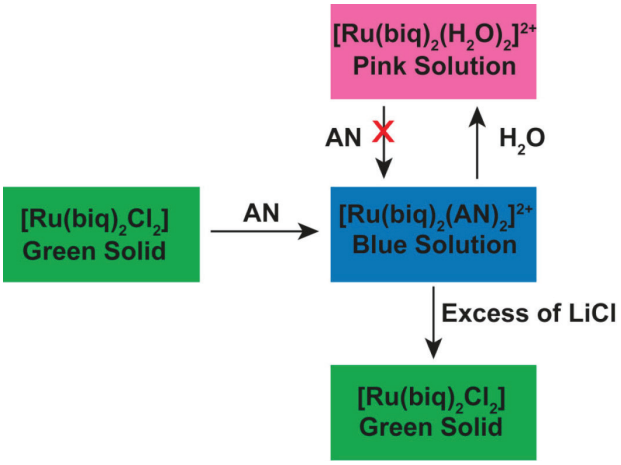

Scheme 1. Solution reactivity of $[Ru(biq)_2Cl_2]$.

Regarding the dark reactivity of nitrosyl **2**, one can verify in Figure 4b that it is inert with respect to NO^+ labilization even in a coordinating solvent, as long as it is kept in the dark. On the other hand, addition of ascorbic acid, a known biological reducing agent, promotes a color change compatible with the formation of the solvated compound $[Ru(biq)_2(AN)_2]^{2+}$ and NO^0, which is then released.[53,61]

Photolysis

Aiming to infer about the photochemical behavior of **2**, we performed irradiation of an acetonitrile solution with continuous light, using a filter for $\lambda_{irrad} < 550$ nm to guarantee visible light irradiation. It is very well documented that coordination of NO^+ to Ru^{II} ion in mononuclear complexes shifts the visible charge transfer absorptions to wavelengths below 400 nm, precluding NO release from direct irradiation with low energy light.[53,61-63] Accordingly, compound **2** has only a residual absorption in the visible region and we were not able to observe significant spectral changes upon irradiation with $\lambda_{irrad} > 550$ nm for up to 3 h (Figure 5a). On the other hand, the same irradiation scheme performed with an equimolar solution of **1** and **2** leads to spectral changes consistent with the formation of the $[Ru(biq)_2(AN)_2]^{2+}$ moiety.

Following previous works of our research group,[20,53] our hypothesis here is that compound **1** can behave as a visible light absorbing chromophore able to trigger NO release from **2** through bimolecular sensitization. The use of a filter for $\lambda_{irrad} < 550$ nm selects the absorption band of **1** or of any solvated species present in solution originated from **1**. The spectra changes depicted in Figure 5b are consistent with this hypothesis, although both compounds **1** and **2** might generate the same photoproduct ($[Ru(biq)_2(AN)_2]^{2+}$, λ_{max} = 604 nm) and the spectrophotometric monitoring suggests NO release only indirectly.

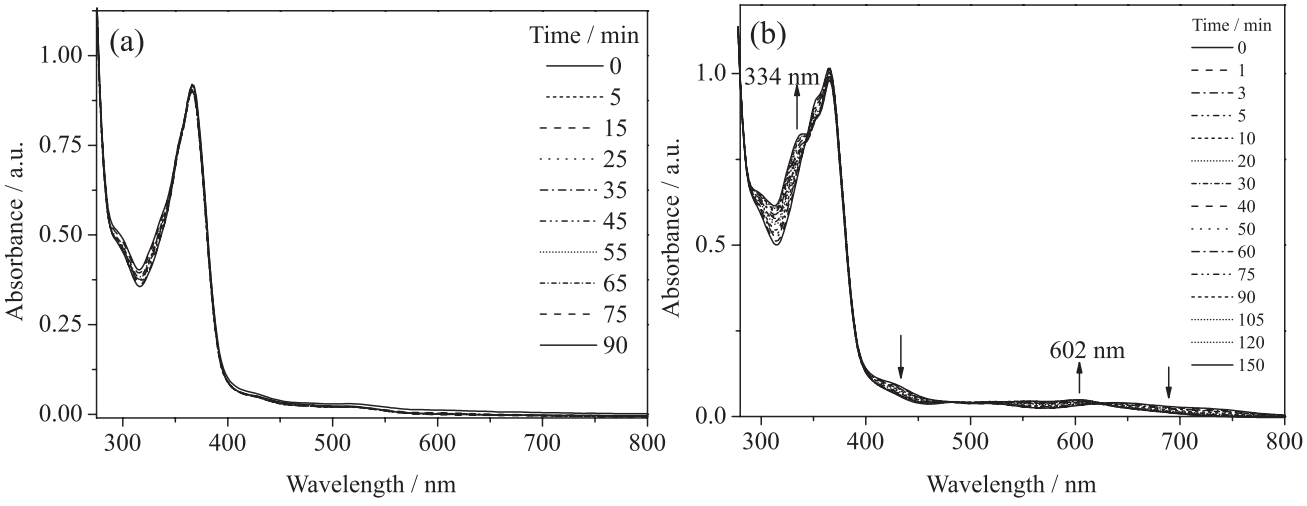

Figure 5. (a) UV-Vis absorption spectra of compound $[Ru(biq)_2(NO)(S)](PF_6)_3$ in acetonitrile solution during irradiation with a Hg lamp using a filter for $\lambda < 550$ nm; (b) photolysis of an equimolar solution of compounds **1** and **2** (acetonitrile, 2×10^{-5} mol L^{-1}), irradiated with a Hg lamp using a filter for $\lambda < 550$ nm.

Therefore, we performed more rigorous experiments using a selective electrode to detect NO^0 in solution by means of amperometric measurements and irradiation with monochromatic (laser) light. The results are shown in Figure 6.

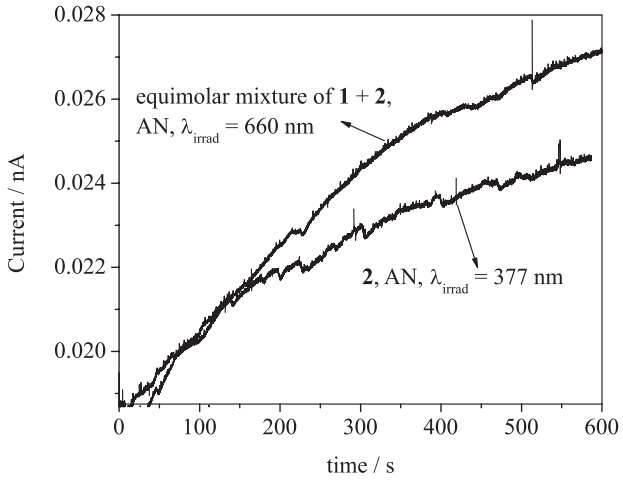

Figure 6. Chronoamperograms of compound **2**, λ_{irrad} = 377 nm, and of an equimolar mixture of compounds **1** and **2**, λ_{irrad} = 660 nm. Both were collected from 1×10^{-4} mol L^{-1} solutions in acetonitrile (AN).

As usual, irradiation of **2** in the UV region (377 nm) causes NO photorelease. Photolysis with visible-light irradiation (660 nm) of a nitrosyl + compound **1** mixture also releases NO, showing that using a $[Ru(biq)_2]$ based chromophore as a photosensitizer is feasible indeed. Surprisingly, for the same concentration of nitrosyl, the sensitized photoreaction was more efficient than that triggered by direct irradiation of the Ru dπ-NO^+ π* charge transfer band at 366 nm (Table 1), as judged by the relative current values observed within the studied time interval (Figure 6). This result is unexpected because a bimolecular collisional process, in diluted solutions, should be less effective.

Solution π-stacking of polyaromatic molecules, even as part of coordination complexes, are documented in the literature.[64,65] The biquinoline ligand, which has planar portions and a π-extended electron cloud is a good site for such weak interactions in solution. Actually, literature[66] reports a precedent showing the stacking of a copper-biquinoline coordination compound. Our photolysis result suggests the formation of a supramolecular assembly held together by weak interacting units of nitrosyl **1** and photosensitizer **2**, possibly due to stacking of some quinoline portion of those molecules. Interacting units would account for the relative high efficiency of the bimolecular sensitized NO photorelease.

Molecular modelling

In order to probe the hypothesis of formation of a supramolecular dimer based on weak interactions, molecular modelling was performed. To do so, we chose the ideal photosensitizer, compound **1**, which has a broad absorption band within the therapeutic window. The optimized geometry of the bimolecular complex is depicted in Figure 7. An interplanar distance of ca. 3.10 Å was seen. This distance is a result of steric hindrance caused by the presence of other ligands from each ruthenium complex. According to our calculations, the Ru–NO bond length is 1.77 Å, which is in accordance with typical Ru–NO bond distances of nitrosyl ruthenium complexes in its singlet ground electronic state.[34,67,68] More importantly, the calculated free energy of the supramolecular assembly formation was predicted to be –8.5 kcal mol^{-1}, which

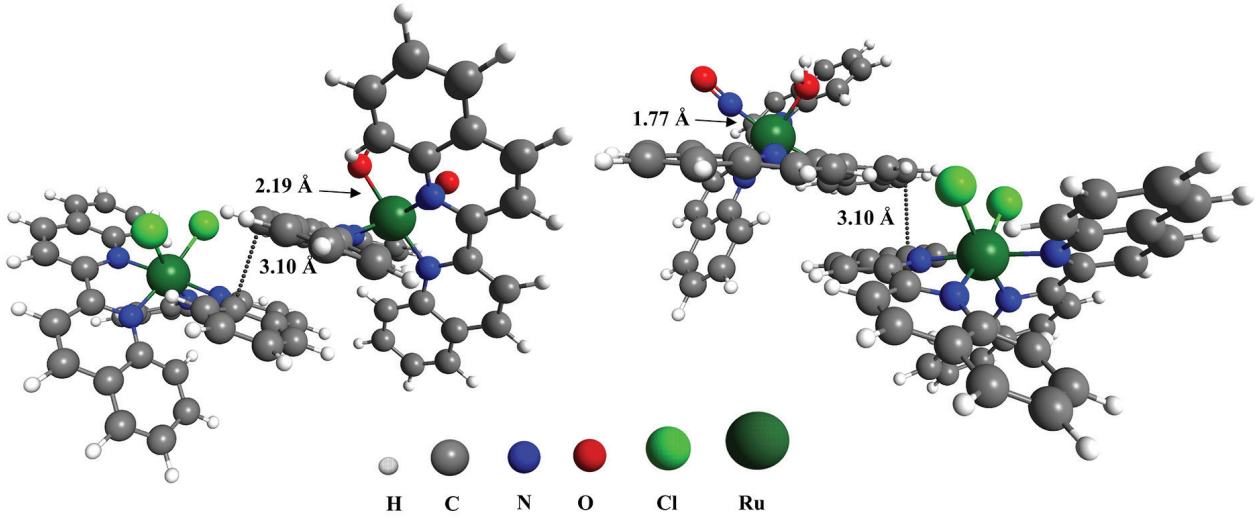

Figure 7. Different views of the DFT/BP86-D3(BJ)/def2-SVP optimized bimolecular structure. For completeness, some key parameters are presented.

indicates that the bimolecular complex is more stable than its separated unimolecular species, i.e., its formation is thermodynamically favored.

To gain further insights into the intermolecular interaction energy of the bimolecular complex, SAPT0 analysis was also performed over the optimized geometry. The SAPT0 results are presented in Table 2.

Table 2. Intermolecular interaction energy for the bimolecular complex calculated by the SAPT0 approach

	SAPT0
E_{Elst} / (kcal mol^{-1})	–54.3
E_{Exch} / (kcal mol^{-1})	52.4
E_{Ind} / (kcal mol^{-1})	–30.2
E_{Disp} / (kcal mol^{-1})	–36.8
E_{SAPT0} / (kcal mol^{-1})	–68.9

SAPT0: zeroth-order symmetry-adapted perturbation theory; E_{Elst}: electrostatics energy; E_{Exch}: exchange energy; E_{Ind}: induction energy; E_{Disp}: dispersion energy; E_{SAPT0}: SAPT0 energy.

According to this approach, electrostatics and dispersion forces play a major role in the interaction within the bimolecular complex, $E_{Elst} = -54.3$, and $E_{Disp} = -36.8$ kcal mol^{-1}, which is fully consistent with the presence of the metal ion and the biquinoline ligand, a relatively large molecule bearing an extended π-cloud. For instance, the London dispersion energy is a long-range electron correlation phenomenon, which is fundamental to molecular adaptability, flexibility, and variety.[69,70] In particular, this force has proven to be crucial in understanding the chemistry and physics of larger structures, for example, a supramolecular assembly such as the one depicted in Figure 7.[71] It is worth pointing out that, although relativistic effects can play a role in stabilizing transition metal systems,[72] the errors associated with the principal approximation used in the SAPT0 model, the many- and one-particle basis sets, determine the overall error of the present calculation. Hence, other small corrections will not improve or change the observed trends. For instance, a previous study[73] involving ruthenium complexes, showed that relativistic corrections for SAPT0 were found to be negligible, therefore, unnecessary to treat these systems.

In the absence of suitable crystals to perform X-ray structural characterization, our DFT results allowed us to analyze the geometry distortion of compounds **1** and **2** claimed to be responsible, in part, for their photoreactivity in solution. As described by the theoretical calculations (Figure 7), there is a distortion of the planes of the crowded bidentate ligands from the 180° dihedral angle expected for their alleged planar structure when coordinated. In compound **1**, the dihedral angles N^1–C^2–C^3–C^5 and N^6–C^7–C^8–C^{10} of biquinoline are 179.6 and 162.2° in the bimolecular system. In contrast, in the nitrosyl substituted portion, the values are 172.5 and 174.6°, respectively, for the N^{11}–C^{12}–C^{13}–C^{15} and N^{16}–C^{17}–C^{18}–C^{20} dihedrals. It is interesting to note that the ligands with the greatest distortion from planarity are precisely those that interact to form the supramolecular assembly (see Figure S7 in Supplementary Information for labels).

In an ideal octahedron, the metal-ligand bond angles are 90°; however, the steric bulk afforded by biquinoline also perturbs the Ru-ligand bond angles of the bimolecular system, which range from 78.2 to 105.4° in each individual species. Hence, this steric strain is expected to contribute to photo-substitution reactions of this complex.

Conclusions

The 2,2'-biquinoline ligand makes the metallic center atypically acidic for a Ru^{II} ion and, in compound **2**, competes for its electron density with the NO^+ ligand. On the other hand, ground state lability of the nitrosyl ion can be triggered by the addition of a reducing agent. These observations, in addition to the high affinity of compounds **1** and **2** for water molecules, are very important because they open the possibility of using compounds like **2** for therapeutic purposes in the dark, without the need for light irradiation.

Besides that, the photolability of biquinoline coordination complexes are observed for compound **1** and it has been atributted mostly to geometry distortions of the octahedral geometry rather than to electronic effects.

Overall, the strategy of bimolecular sensitization of NO release with visible low energy light was successful. However, due to the high lability of the chloro ligands introduced by the steric bulk biquinoline ligand in compound **1**, the actual photosensitizer was the solvated complex $[Ru(biq)_2(AN)_2]^{2+}$. On the other hand, our molecular modelling suggests the occurrence of a supramolecular assembly in solution between compounds **1** and **2**, which would improve the photosensitization both in terms of efficiency (due to the weak interaction between the chromophores) and the higher irradiation wavelength. Therefore, considering compound **1** as an ideal photosensitizer, this work should continue focusing strategies to control the lability of the chloro ligands and to assure the occurrence and maintenance of the supramolecular assembly. These strategies will address the investigations of solutions containing Cl^- anions, ideally in physiological concentrations, and the use of formulations such as liposomes.

Supplementary Information

Supplementary information (a scheme of the apparatus used in the amperometric detection of NO; mass spectra of **1** and **2**; IR spectrum of **2**; voltammograms of **2**; labeling for the theoretical structure for the supramolecular dimer) is available free of charge at http://jbcs.sbq.org.br as PDF file.

Acknowledgments

This work was supported by the Brazilian agencies FAPESP (Fundação de Amparo à Pesquisa do Estado de São Paulo) (grant 2018/18060-3) and financed in part by the Coordenação de Pessoal de Nível Superior (CAPES), finance code 001. Authors also would like to thank Prof Roberto Santana da Silva for the use of the NOmeter.

References

1. Fukuzumi, S.; Kojima, T.; Lee, Y. M.; Nam, W.; *Coord. Chem. Rev.* **2017**, *333*, 44.
2. Wu, L.; Nayak, A.; Shao, J.; Meyer, T. J.; *Proc. Natl. Acad. Sci. U. S. A.* **2019**, *166*, 11153.
3. Concepcion, J. J.; Jurss, J. W.; Brennaman, M. K.; Hoertz, P. G.; Patrocinio, A. O. T.; Iha, N. Y. M.; Templeton, J. L.; Meyer, T. J.; *Acc. Chem. Res.* **2009**, *42*, 1954.
4. Grabulosa, A.; Beley, M.; Gros, P. C.; Cazzanti, S.; Caramori, S.; Bignozzi, C. A.; *Inorg. Chem.* **2009**, *48*, 8030.
5. Veiga, E. T.; Müller, A. V.; Ramos, L. D.; Frin, K. P. M.; Polo, A. S.; *Eur. J. Inorg. Chem.* **2018**, *2018*, 2680.
6. Balzani, V.; Juris, A.; *Coord. Chem. Rev.* **2001**, *211*, 97.
7. Vögtle, F.; Plevoets, M.; Nieger, M.; Azzellini, G. C.; Credi, A.; de Cola, L.; de Marchis, V.; Venturi, M.; Balzani, V.; *J. Am. Chem. Soc.* **1999**, *121*, 6290.
8. Li, A.; Turro, C.; Kodanko, J. J.; *Acc. Chem. Res.* **2018**, *51*, 1415.
9. Heinemann, F.; Karges, J.; Gasser, G.; *Acc. Chem. Res.* **2017**, *50*, 2727.
10. Knoll, J. D.; Albani, B. A.; Turro, C.; *Acc. Chem. Res.* **2015**, *48*, 2280.
11. Hoertz, P. G.; Staniszewski, A.; Marton, A.; Higgins, G. T.; Incarvito, C. D.; Rheingold, A. L.; Meyer, G. J.; *J. Am. Chem. Soc.* **2006**, *128*, 8234.
12. Toledo, J. C.; Augusto, O.; *Chem. Res. Toxicol.* **2012**, *25*, 975.
13. Cheng, J.; He, K.; Shen, Z.; Zhang, G.; Yu, Y.; Hu, J.; *Front. Chem.* **2019**, *7*, DOI 10.3389/fchem.2019.00530.
14. Yang, T.; Zelikin, A. N.; Chandrawati, R.; *Adv. Sci.* **2018**, *5*, 1701043.
15. Naghavi, N.; de Mel, A.; Alavijeh, O. S.; Cousins, B. G.; Seifalian, A. M.; *Small* **2013**, *9*, 22.
16. Yu, Y.; Xu, Q.; He, S.; Xiong, H.; Zhang, Q.; Xu, W.; Ricotta, V.; Bai, L.; Zhang, Q.; Yu, Z.; Ding, J.; Xiao, H.; Zhou, D.; *Coord. Chem. Rev.* **2019**, *387*, 154.
17. da Silva, C. F. N.; Possato, B.; Franco, L. P.; Ramos, L. C. B.; Nikolaou, S.; *J. Inorg. Biochem.* **2018**, *186*, 197.
18. Cacita, N.; Possato, B.; da Silva, C. F. N.; Paulo, M.; Formiga, A. L. B.; Bendhack, L. M.; Nikolaou, S.; *Inorg. Chim. Acta* **2015**, *429*, 114.
19. Carneiro, Z. A.; Biazzotto, J. C.; Alexiou, A. D. P.; Nikolaou, S.; *J. Inorg. Biochem.* **2014**, *134*, 36.
20. Fornari, E. C.; Marchesi, M. S. P.; Machado, A. E. H.; Nikolaou, S.; *Polyhedron* **2009**, *28*, 1121.
21. de Carvalho, A. N.; Fornari, E. C.; Gomes, W. R.; Araújo, D. M. S.; Machado, A. E. H.; Nikolaou, S.; *Inorg. Chim. Acta* **2011**, *370*, 444.
22. Keyes, T. E.; Vos, J. G.; Kolnaar, J. A.; Haasnoot, J. G.; Reedijk, J.; Hage, R.; *Inorg. Chim. Acta* **1996**, *245*, 237.
23. Diamantis, A. A.; Dubrawski, J. V.; *Inorg. Chem.* **1981**, *20*, 1142.
24. Frisch, M. J.; Trucks, G. W.; Schlegel, H. B.; Scuseria, G. E.; Robb, M. A.; Cheeseman, J. R.; Scalmani, G.; Barone, V.; Mennucci, B.; Petersson, G. A.; Nakatsuji, H.; Caricato, M.; Li, X.; Hratchian, H. P.; Izmaylov, A. F.; Bloino, J.; Zheng, G.; Sonnenberg, J. L.; Hada, M.; Ehara, M.; Toyota, K.; Fukuda, R.; Hasegawa, J.; Ishida, M.; Nakajima, T.; Honda, Y.; Kitao, O.; Nakai, H.; Vreven, T.; Montgomery Jr., J. A.; Peralta, J. E.; Ogliaro, F.; Bearpark, M.; Heyd, J. J.; Brothers, E.; Kudin, K. N.; Staroverov, V. N.; Kobayashi, R.; Normand, J.; Raghavachari, K.; Rendell, A.; Burant, J. C.; Iyengar, S. S.; Tomasi, J.; Cossi, M.; Rega, N.; Millam, J. M.; Klene, M.; Knox, J. E.; Cross, J. B.; Bakken, V.; Adamo, C.; Jaramillo, J.; Gomperts, R.; Stratmann, R. E.; Yazyev, O.; Austin, A. J.; Cammi, R.; Pomelli, C.; Ochterski, J. W.; Martin, R. L.; Morokuma, K.; Zakrzewski, V. G.; Voth, G. A.; Salvador, P.; Dannenberg, J. J.; Dapprich, S.; Daniels, A. D.; Farkas, Ö.; Foresman, J. B.; Ortiz, J. V; Cioslowski, J.; Fox, D. J.; *Gaussian 09*, *Revision D.01*; Gaussian Inc., Wallingford, CT, USA, 2009.
25. Becke, A. D.; *Phys. Rev. A* **1988**, *38*, 3098.
26. Perdew, J. P.; *Phys. Rev. B* **1986**, *33*, 8822.
27. Grimme, S.; Ehrlich, S.; Goerigk, L.; *J. Comput. Chem.* **2011**, *32*, 1456.
28. Weigend, F.; Ahlrichs, R.; *Phys. Chem. Chem. Phys.* **2005**, *7*, 3297.
29. Escudero, D.; Thiel, W.; Champagne, B.; *Phys. Chem. Chem. Phys.* **2015**, *17*, 18908.
30. Anusha, C.; De, S.; Parameswaran, P.; *Dalton Trans.* **2013**, *42*, 14733.
31. Lastra-Barreira, B.; Díez, J.; Crochet, P.; Fernández, I.; *Dalton Trans.* **2013**, *42*, 5412.
32. Śliwa, P.; Handzlik, J.; Czeluśniak, I.; *J. Organomet. Chem.* **2014**, *767*, 6.

33. Aoto, Y. A.; Batista, A. P. L.; Köhn, A.; de Oliveira-Filho, A. G. S.; *J. Chem. Theory Comput.* **2017**, *13*, 5291.
34. Batista, A. P. L.; de Oliveira-Filho, A. G. S.; Galembeck, S. E.; *Phys. Chem. Chem. Phys.* **2017**, *19*, 13860.
35. Marenich, A. V.; Cramer, C. J.; Truhlar, D. G.; *J. Phys. Chem. B* **2009**, *113*, 6378.
36. Grimme, S.; *Chem. - Eur. J.* **2012**, *18*, 9955.
37. Luchini, G.; Alegre-Requena, J.; IFunes; Rodríguez-Guerra, J.; Chen, J.; Paton, R.; *bobbypaton/GoodVibes: GoodVibes*, v3.0.0; Zenodo, Switzerland, 2019.
38. Hohenstein, E. G.; Sherrill, C. D.; *J. Chem. Phys.* **2010**, *132*, 184111.
39. Hohenstein, E. G.; Parrish, R. M.; Sherrill, C. D.; Turney, J. M.; Schaefer III, H. F.; *J. Chem. Phys.* **2011**, *135*, 174107.
40. Parker, T. M.; Burns, L. A.; Parrish, R. M.; Ryno, A. G.; Sherrill, C. D.; *J. Chem. Phys.* **2014**, *140*, 094106.
41. Hohenstein, E. G.; Sherrill, C. D.; *WIREs Comput. Mol. Sci.* **2012**, *2*, 304.
42. Parrish, R. M.; Burns, L. A.; Smith, D. G. A.; Simmonett, A. C.; DePrince, A. E.; Hohenstein, E. G.; Bozkaya, U.; Sokolov, A. Y.; Di Remigio, R.; Richard, R. M.; Gonthier, J. F.; James, A. M.; McAlexander, H. R.; Kumar, A.; Saitow, M.; Wang, X.; Pritchard, B. P.; Verma, P.; Schaefer, H. F.; Patkowski, K.; King, R. A.; Valeev, E. F.; Evangelista, F. A.; Turney, J. M.; Crawford, T. D.; Sherrill, C. D.; *J. Chem. Theory Comput.* **2017**, *13*, 3185.
43. Hellweg, A.; Hättig, C.; Höfener, S.; Klopper, W.; *Theor. Chem. Acc.* **2007**, *117*, 587.
44. Weigend, F.; *J. Comput. Chem.* **2008**, *29*, 167.
45. Bode, B.; Gordon, M. S.; *J. Mol. Graph. Mod.* **1998**, *16*, 133.
46. Henderson, W.; McIndoe, J. S.; *Mass Spectrometry of Inorganic, Coordination and Organometallic Compounds*; John Wiley & Sons, Ltd.: Chichester, 2005.
47. Ueno, K.; Imamura, T. In *Handbook of Organic Analytical Reagents*; Ueno, K.; Imamura, T.; Cheng, K. L., eds.; CRC Press: Boca Raton, 1992, p. 393.
48. Nakamoto, K.; *Infrared and Raman Spectra of Inorganic and Coordination Compounds: Part A: Theory and Applications in Inorganic Chemistry*, 6th ed.; Wiley: Milwaukee, 2008.
49. Sauaia, M. G.; da Silva, R. S.; *Transition Met. Chem.* **2003**, *28*, 254.
50. Juris, A.; Balzani, V.; *Coord. Chem. Rev.* **1988**, *84*, 85.
51. Dongare, P.; Myron, B. D. B.; Wang, L.; Thompson, D. W.; Meyer, T. J.; *Coord. Chem. Rev.* **2017**, *345*, 86.
52. Campagna, S.; Puntoriero, F.; Nastasi, F.; Bergamini, G.; Balzani, V. In *Photochemistry and Photophysics of Coordination Compounds I*; Balzani, V.; Campagna, S., eds.; Springer: Berlin, 2007, p. 117-214.
53. Tfouni, E.; Truzzi, D. R.; Tavares, A.; Gomes, A. J.; Figueiredo, L. E.; Franco, D. W.; *Nitric Oxide* **2012**, *26*, 38.
54. Knoll, J. D.; Albani, B. A.; Durr, C. B.; Turro, C.; *J. Phys. Chem. A* **2014**, *118*, 10603.
55. Zhao, J.; Liu, N.; Sun, S.; Gou, S.; Wang, X.; Wang, Z.; Li, X.; Zhang, W.; *J. Inorg. Biochem.* **2019**, *196*, 110684.
56. Battistin, F.; Balducci, G.; Wei, J.; Renfrew, A. K.; Alessio, E.; *Eur. J. Inorg. Chem.* **2018**, *2018*, 1469.
57. Wachter, E.; Heidary, D. K.; Howerton, B. S.; Parkin, S.; Glazer, E. C.; *Chem. Commun.* **2012**, *48*, 9649.
58. Woods, J. J.; Cao, J.; Lippert, A. R.; Wilson, J. J.; *J. Am. Chem. Soc.* **2018**, *140*, 12383.
59. Albani, B. A.; Whittemore, T.; Durr, C. B.; Turro, C.; *Photochem. Photobiol.* **2015**, *91*, 616.
60. Barigelletti, F.; Juris, A.; Balzani, V.; Belser, P.; von Zelewsky, A.; *Inorg. Chem.* **1983**, *22*, 3335.
61. Mir, J. M.; Malik, B. A.; Maurya, R. C.; *Rev. Inorg. Chem.* **2019**, *39*, 91.
62. Doro, F. G.; Ferreira, K. Q.; da Rocha, Z. N.; Caramori, G. F.; Gomes, A. J.; Tfouni, E.; *Coord. Chem. Rev.* **2016**, *306*, 652.
63. Cândido, M. C. L.; Oliveira, A. M.; Silva, F. O. N.; Holanda, A. K. M.; Pereira, W. G.; Sousa, E. H. S.; Carneiro, Z. A.; Silva, R. S.; Lopes, L. G. F.; *J. Braz. Chem. Soc.* **2015**, *26*, 1824.
64. Zhong, C. J.; Kwan, W. S. V.; Miller, L. L.; *Chem. Mater.* **1992**, *4*, 1423.
65. Toma, S. H.; Uemi, M.; Nikolaou, S.; Tomazela, D. M.; Eberlin, M. N.; Toma, H. E.; *Inorg. Chem.* **2004**, *43*, 3521.
66. Martínez, N. P.; Isaacs, M.; Oliver, A. G.; Ferraudi, G.; Lappin, A. G.; Guerrero, J.; *Dalton Trans.* **2018**, *47*, 13171.
67. Vidal, R. D. S.; Doro, F. G.; Ferreira, K. Q.; da Rocha, Z. N.; Castellano, E. E.; Nikolaou, S.; Tfouni, E.; *Inorg. Chem. Commun.* **2012**, *15*, 93.
68. Caramori, G. F.; Kunitz, A. G.; Andriani, K. F.; Doro, F. G.; Frenking, G.; Tfouni, E.; *Dalton Trans.* **2012**, *41*, 7327.
69. Grimme, S.; *WIREs Comput. Mol. Sci.* **2011**, *1*, 211.
70. Liptrot, D. J.; Power, P. P.; *Nat. Rev. Chem.* **2017**, *1*, 0004.
71. Wagner, J. P.; Schreiner, P. R.; *Angew. Chem., Int. Ed.* **2015**, *54*, 12274.
72. Macleod-Carey, D.; Caramori, G. F.; Guajardo-Maturana, R.; Paez-Hernandez, D.; Muñoz-Castro, A.; Arratia-Perez, R.; *Int. J. Quantum Chem.* **2019**, *119*, e25777.
73. Galembeck, S. E.; Caramori, G. F.; Misturini, A.; Garcia, L. C.; Orenha, R. P.; *Organometallics* **2017**, *36*, 3465.

Submitted: January 14, 2020
Published online: May 15, 2020